31st Annual International Conference of the IEEE EMBS
Minneapolis, Minnesota, USA, September 2-6, 2009

Method to Quantify the Effect of Passivation Layer in Bio-Impedance Sensors

Shree Narayanan*, Mehdi Nikkhah*, Jeannine S. Strobl, and Masoud Agah

***Abstract*—This paper investigates the effect of the passivation layer in a bio-impedance sensor. A sensor with 20 sensing sites has been designed, fabricated using a simple two mask process and tested. We have cultured *in-vivo* MDA-MB231 mammary cells and recorded the impedance from 1kHz to 1MHz. Processing the recorded data brings to light the drawback of the passivation layer which results in a drop in sensitivity of 13%. Simulation results based on parameters extracted from measurements re-affirm the drop in sensitivity. Thus, the passivation layer needs to be provided a special consideration in future design of the sensor as it can modify the response of the sensor.**

I. Introduction

BIO-IMPEDANCE micro sensors can sense the presence of cells by planar impedance measurement [1]. The most common among this is two-electrode measurement technique [2]. They are non-invasive [3], and can provide the luxury of having simultaneous multi-site detection [4] due to their small size. Hence, it has been used quite frequently [5]-[8] to detect the presence of cells. In this simple technique, cultured cells adhere onto planar fabricated micro-electrodes and the impedance between two such electrodes is measured. Most essential in the design of these sensors is the passivation layer. As the name suggests, this layer is used to isolate the contact of the cells to the unwanted regions of electrodes. This layer has been commonly used in previously developed sensors [5]-[8]. Completely passivated sensors have also been used to measure the impedance without any galvanic contact [9]-[10]. Photoresist has been used in the past, in many sensor designs, to perform this role, for the ease of integration with the fabrication process flow [11]. However, not enough attention has been given to the effect it could have on the impedance measurement and the sensitivity of the sensor. In this paper, we have designed a novel bio-impedance micro-sensor with 20 sensing sites to address the effect of the passivation layer on the sensitivity of sensor. Investigations using this sensor indicate that the un-ideal passivation layer, an important component of this sensor can decrease the sensitivity. Our simulations based on an equivalent circuit model also reveal such a drop in the sensitivity.

Manuscript received June 19, 2009. Shree Narayanan, is a Graduate student in Virginia Tech MEMS Laboratory, The Bradley Department of Electrical and Computer Engineering, Virginia Tech, Blacksburg, VA 24060 USA

Mehdi Nikkhah is with the Mechanical Engineering Department and also Virginia Tech MEMS Laboratory.

Jeannine S. Strobl is with the Edward Via Virginia College of Osteopathic Medicine, Blacksburg, VA, 24060.

Masoud Agah is with the Virginia Tech MEMS Laboratory, Virginia Tech, Blacksburg, VA, 24061 (corresponding author: Shree Narayanan, phone: 540-231-4180; fax: 540-231-3362; e-mail: snsnair@vt.edu).

* These authors equally contributed to this work

II. Theory

A. Sensor Structure

As stated earlier, a bio-impedance sensor consists of planar fabricated micro-electrodes. These electrodes are exposed to a culture medium which is contained within an enclosure such as a cloning cylinder. Fig 1 shows a conceptual structure. The sensing window and the passivated areas form the two different electrical paths whose parallel impedance is measured.

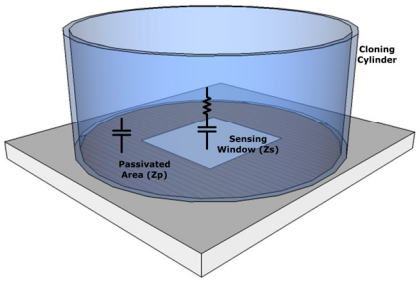

$$Z_{measured} = Z_s \,||\, Z_p \qquad (1)$$

The measured impedance is dependent on the area of the electrode exposed to the medium [12]. Hence, the passivation layer defines the "sensing window" and ideally eliminates the effect of cells adhered on its surface in the measured impedance. In other words, it causes the measured impedance to be attributed only to those cells adhered on the electrodes in the sensing window. The passivation layer can be used to define multiple sensing sites which will be helpful when detecting low density culture.

B. Electrical model

The underlying principle is that cells in the medium adhere onto the electrodes and increase the measured impedance. Ideally, we would expect the sensor to be sensitive only to cells in the sensing window. However, the

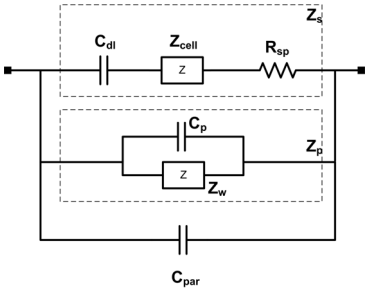

Fig 2: Electrical model representing the sensor

parallel electrical path through the passivation layer alters the response, decreasing the sensitivity in the process. A circuit model representing the sensor is shown in Fig 2.

Z_s is the impedance measured in the sensing window which consists of the double-layer capacitance (C_{dl}) in series with the spreading resistance (R_{sp}) [12]. This is the simplified Randles model [15]. In addition, when cells are introduced, there is an additional Z_{cell}. The passivation layer is implemented by using a photoresist in our sensor. This offers capacitance (C_p) and Warburg impedance (Z_w) [13]. The additional component due to cells adhered onto the passivation layer has not been shown for the sake of simplicity. There is also a parasitic capacitance (C_{par}) which is dominant when the frequency becomes close to 1MHz. These capacitances have been modeled as CPEs based on the measurements obtained which showed a constant phase angle at low frequencies [14].

III. Fabrication and Setup

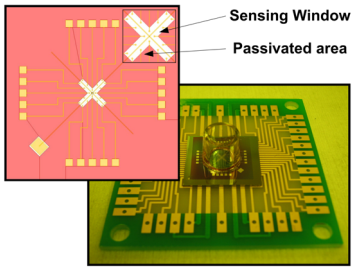

Fig 3: Design configuration of the proposed micro electrodes. The right top inset shows the sensor sensing area.

Fig 3 shows the layout of the biosensor and the fabricated biochip assembled on a printed circuit board (PCB). The chip consists of multiple electrodes with the return electrode passing symmetrically among them. The width of each individual electrode is 30µm with a circular tip of 45µm in radius. Each electrode is accompanied with a 500µm square pad for electrical interface. Fabrication process starts by depositing 5000Å-thick oxide layer on a silicon wafer followed by evaporation of 300Å/500Å Cr/Au on the oxide layer. The wafer was then spun coated with approximately 6µm of photoresist (9260). After patterning the photoresist, the Au layer was electroplated to a thickness of ~2.5µm. The photoresist was removed and subsequently the Au and Cr seed layers were etched. A second photoresist

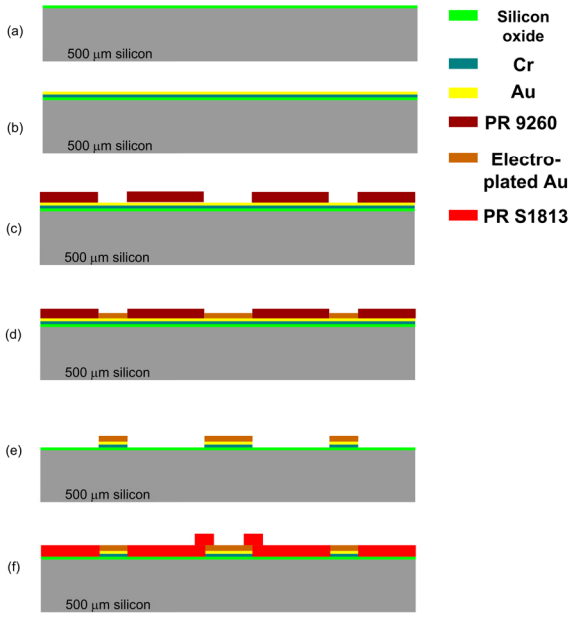

Fig 4: Two-mask fabrication process of the MEMS sensor.

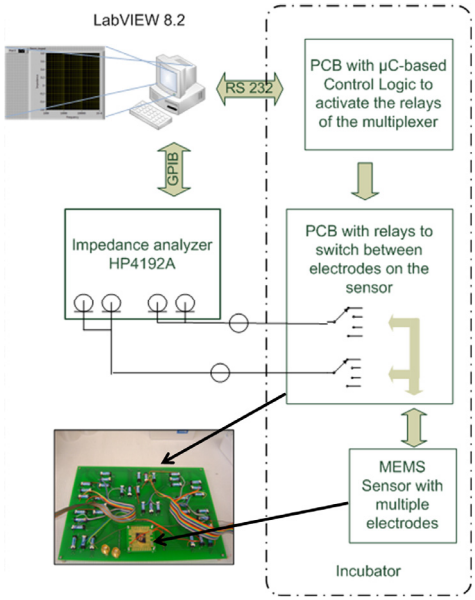

Fig 5: Block diagram of the measurement setup with the picture of the multiplexing circuitry.

(passivation) layer (S1813) was spun on the wafer and was patterned to open the sensing window. The process flow is shown in Fig 4.

The measurement setup, shown in Fig 5, consists of a self-built computer-controlled multiplexer to switch the corresponding electrodes from the sensor to an impedance analyzer. A program in LabVIEW was used to switch the electrodes and to sweep through logarithmic frequencies from 1kHz to 1MHz every 30min. The absolute impedances of medium with and without cells (Z_c and Z_m) and normalized impedance, Γ were stored programmatically over a period of 24 hours, once every half an hour. The normalized impedance Γ is defined as in

$$\Gamma = \frac{(Z_c - Z_m)}{Z_m} \quad (2)$$

In this work, MDA-MB-231 human breast cancer cells were incubated in standard culture medium at 37ºC and 7% CO_2 during experimentation. A high initial seeding density of $20x10^4$/250µl was used for experiments.

IV. Experiment

First, the impedance of the cells, Z_1 was measured with the sensing area uncovered (Case I). The measurement was performed over a period of 24 hours, once every half an hour. It should be noted that the first measurement corresponds to cell culture medium without any cells $Z_{m1}=Z_{pm1}||Z_{sm1}$. Once cells are added, the values measured correspond to $Z_{c1}=Z_{pc1}||Z_{sc1}$. Hence, when calculating Γ_1, the impedance due to the passivated area (Z_p) also plays a role.

$$\Gamma_1 = \frac{(Z_{pc1} \,||\, Z_{sc1}) - (Z_{pm1} \,||\, Z_{sm1})}{(Z_{pm1} \,||\, Z_{sm1})} \quad (3)$$

To filter out Z_p we consider Case II, in which the sensing window is also fully covered with the passivation layer (i.e. photoresist). In this case, we record value $Z_2=Z_{p2}$. This is because there is no open sensing window in this case. The sensing window has been calculated to occupy just 10% of the total area, therefore

$$Z_{p1} = 1.1Z_{p2} = 1.1Z_2 \quad (4)$$

This is because Z_{p1} and Z_{p2} are similar impedances but of different area. These set of measurements will also yield Z_{m2} and Z_{c2} similar to the previous case. Thus, from (4) we can determine Z_{p1}. This method of filtering out the passivation impedance is performed for both impedances, with and without cells. These new set of values give rise to Γ_2 which is the normalized impedance when an ideal passivation layer is used.

$$\Gamma_2 = \frac{(Z_{sc1} - Z_{sm1})}{Z_{sm1}} \quad (5)$$

V. Results

Fig 6 shows the SEM and optical images of cells cultured on the sensor after 24 hours showing the attachment and spreading of the cells on the sensing area. Since there are measurements from 12 sensing sites, the average of all these measurements has been used for processing. This minimizes the effect of the variation in the biological domain of the experiment. Fig 7 plots the average measurement of the impedance of the medium and the standard deviation in the measurement.

Fig 8 shows a plot of the normalized measured impedances from measured values after 2 hours, processed as explained in (3)-(5). The peak around 100 kHz, in Fig 8, corresponds to the presence of cells in the measurement.

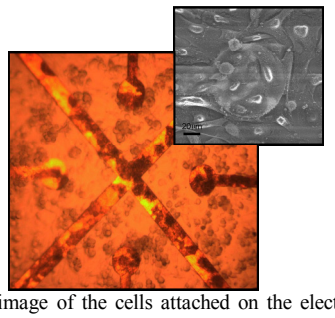

Fig 6: Optical image of the cells attached on the electrodes. Top right image shows the SEM image of the cancer cells attached on a single electrode.

Cells adhere onto the electrodes through focal points on the surface underneath. Elsewhere, there is a small gap between the cell surface and the electrodes. This area which is in contact with the electrodes has been estimated to be 6µm^2 [16]. This electrically resistive gap in parallel with the cell

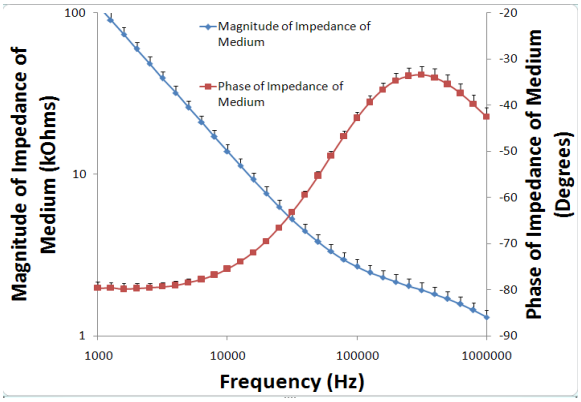

Fig 7: Average of measured values of Zm_1 and the standard deviation

capacitance tends to increase the measured impedance to around 100 kHz [12]. This increase is observed as a peak in Fig 8. Further, at the low frequencies, the decrease in the impedance has been ascribed to the proteins metabolized by the cells [11]. With and without Z_p taken into calculation, i.e. Γ_1 and Γ_2 respectively differ by 13% for this sensor. Further, one can notice the slight shift in the frequency at which the peak occurs. In this case, it decreased from 125 kHz to 100 kHz due to the presence of the passivation layer. These are some of the issues with using a passivation layer in the bio-sensor.

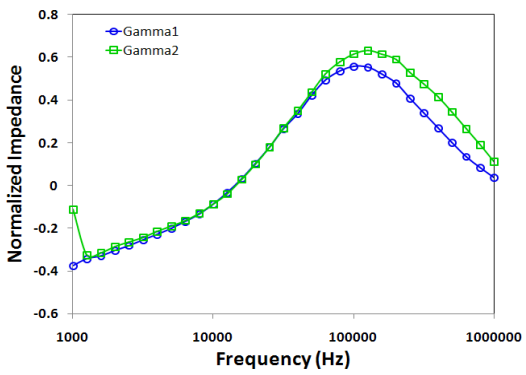

Fig 8: Experimental values of Γ_1 and Γ_2 obtained from measurements

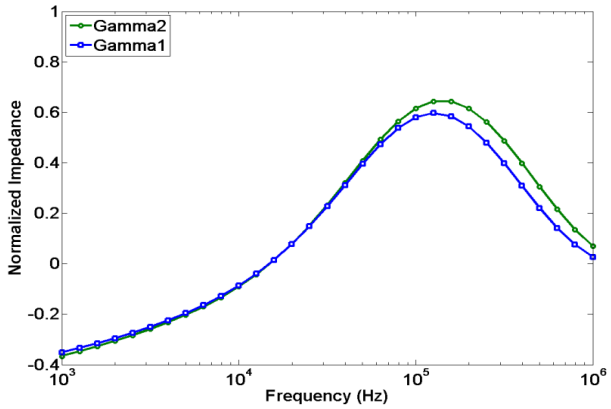

Fig 9: Values of Γ_1 and Γ_2 obtained from simulations. The parameters were extracted from the measurements to fit the circuit model.

We now model the sensors in Case I and II in terms of the circuit model in Fig 2. We now obtain a MATLAB simulation of the impedance of circuit model in Fig 9 which was performed with and without the presence of the passivation layer impedance Z_p. The values for the parameters were obtained from the measurements and the processing explained in Section IV. This simulation, though does not take into account the presence of cells on the passivation layer, shows the trend that has previously been observed in Fig 8.

The reason for this drop in sensitivity can be reasoned from the manner in which the impedances Z_s and Z_p vary with increasing frequency. In Fig 10, the variation in Z_s and Z_p which are approximated to the impedance in Case I and II, respectively, are plotted. The entire frequency range can be broken down into two regions as shown. In region 1, Z_p

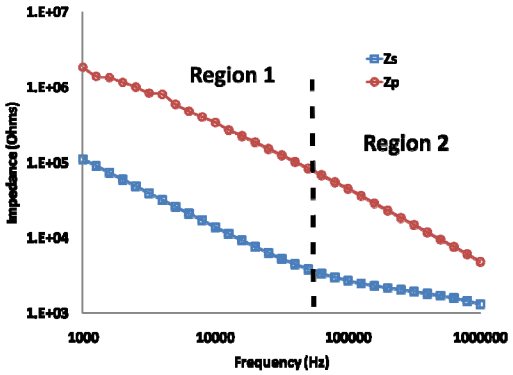

Fig 10: Variation of medium (~Zs) and passivated layer impedance (~Zp)

is an order of magnitude greater than Z_s. However, in region 2, as Z_s enters the resistive regime wherein, spreading resistance R_{sp} dominates C_{dl}, the difference between Z_s and Z_p tends to diminish with increasing frequency. It is this decrease which causes Z_p to play a much more dominant role, reducing the measured impedance and thereby decreasing sensitivity at higher frequencies.

VI. CONCLUSION

We have shown that the presence of passivation layer has caused a drop of 13% in sensitivity of the proposed sensor. Furthermore, the peak frequency has been affected by the presence of this un-ideal layer and the cells that adhere on it. Thus, we can conclude that future work towards the design of such biosensors will need to address these issues, in order to sense low density cell populations efficiently. One possibility is to use a thicker photoresist layer or to use a different material that has a lower dielectric constant (better insulator). To address the issue of bio-compatibility one can also have a thick layer of low dielectric constant material which is covered by a relatively thin layer of bio-compatible material. This multi-passivation layer stack can also provide high impedance.

REFERENCES

[1] Paramitra Mitra, Charles R. Keese, and Ivar Giaever, "Electric measurements can be used to monitor the attachment and spreading of cells in tissue culture," *BioTechniques*, vol. 11, Issue 4, 504–510, 1991.

[2] R. Bragos, E. Sarro, A. Fontova, A. Soley, J. Cairo, A. Bayes-Genis, and J. Rosell, "Four Versus Two-Electrode Measurement Strategies for Cell Growing and Differentiation Monitoring Using Electrical Impedance Spectroscopy," *Proc. of the 28th IEEE EMBS Annual International Conference*, New York City, USA, Aug 30-Sept 3, 2006.

[3] Joachim Wegener, Charles R. Keese, and Ivar Giaever, "Electric cell-substrate impedance sensing (ECIS) as a noninvasive means to monitor the kinetics of cell spreading to artificial surfaces," *Experimental cell research*, vol. 259, Issue 1, 158, 2000.

[4] Xiaoqiu Huang, I. Nausieda, D. W. Greve, M. M. Domach, D. Nguyen, "Development of active matrix biosensor array for cell screening," *Sensors, 2004. Proceedings of IEEE*, pp. 72-75 vol.1, 24-27 Oct. 2004.

[5] Ivar Giaever and Charles R. Keese, "Micromotion of mammalian cells measured electrically," *Proc. of the National Academy of Sciences of the United States of America*, vol.88, Issue 17, 7896, Oct. 1991.

[6] Xiaoqiu Huang, Duc Nguyen, Michael M. Domach, and David W. Greve, "Impedance based biosensor for monitoring mammalian cell behavior," *Proc. of IEEE Sensor,* pp. 304-309, 2003.

[7] R. Ehret, W. Baumann, M. Brischwein, A. Schwinde, K. Stegbauer, B. Wolf, "Monitoring of cellular behaviour by impedance measurements on interdigitated electrode structures", *Biosensors & bioelectronic*, vol. 12, issue 1, 29, 1997.

[8] D. Borkholder, "Cell based biosensors using micro electrodes," Ph.D. dissertation, Dept. Elect. Eng., Stanford Univ., Palo Alto, CA, 1998.

[9] M.C. Hofmann, D. Ellersiek, F. Kensy, J. Buchs, W. Mokwa, U. Schnakenberg, "Galvanic decoupled sensor for monitoring biomass concentration during fermentation processes," *Sensors and actuators. B, Chemical*, vol. 111-112, pp. 370, 2005.

[10] M. C. Hofmann, R. Schlierf, W. Mokwa, U. Schnakenberg, F. Kensy, and J. Buchs, "Galvanically decoupled impedance spectroscopy for biological high-throughput-screening in microtiter plates," *Sensors, 2005 IEEE*, pp.4, Oct. 30 2005-Nov. 3 2005.

[11] D. T. Price, A. R. A. Rahman, S. Bhansali, "Design rule for optimization of microelectrodes used in electric cell-substrate impedance sensing (ECIS)", *Biosensors & bioelectronics,* vol. 24, Issue 7, 2071, 2009.

[12] Xiaoqiu Huang, Duc Nguyen, D. W. Greve, and M. M. Domach, "Simulation of microelectrode impedance changes due to cell growth," *Sensors Journal, IEEE*, vol.4, no.5, pp. 576-583, Oct. 2004.

[13] D. M., Taylor and A. G. McDonald, "AC admittance of the metal/insulator/electrolyte interface," *Journal of physics. D, Applied physics*, vol. 20, Issue 10, pp. 1277, 2000.

[14] Sverre Grimnes and Orjan G. Martinsen, *BioImpedance and BioElectricity Basics.* Boston, MA: Elsevier Academic Press, 2008, pp. 123–135.

[15] K. L. Roach, "Electrochemical Models for Electrode Behavior in Retinal Prosthesis," M. Eng. Report, Dept. Elect. Eng. And Comp. Sci., Massachusetts Institute of Technology, Cambridge, MA, 2003.

[16] P. F. Davis, A. Robotewskyj, and M. L. Griem, "Endothelial cell adhesion in real time. Measurements in vitro by tandem scanning confocal image analysis," *J. Clin. Invest.*, vol. 91, pp. 2640–2652, 1991